

# Design of a Silicon-Plasmonic Hybrid Electro-Optic Modulator

Mu Xu, Jiayang Wu, Zhiming Zhuang, Fei Li, Tao Wang, Linjie Zhou, and Yikai Su

State Key Lab of Advanced Optical Communication Systems and Networks, Department of Electronic Engineering, Shanghai Jiao Tong University, Shanghai 200240, China, E-mail: yikaisu@sjtu.edu.cn

**Abstract**— We propose a racetrack ring based optical modulator employing an electro-optic polymer infiltrated silicon-plasmonic hybrid phase shifter. From simulation results, an extinction ratio of higher than 15 dB is achieved at 1550-nm wavelength under a 1.2-V bias. A modulation bandwidth of more than 100 GHz can be potentially obtained due to a fast response speed of the Pockels effect, a reduced  $RC$  delay, and a decreased quality factor of the ring.

**Keywords**- hybrid, silicon photonics, plasmonics, racetrack ring resonators

## I. INTRODUCTION

The achievable bandwidths of free carrier dispersion (FCD) based silicon modulators are limited by two-photon generated free carrier effects [1] and  $RC$  time constants [2], [3]. As a possible solution to overcome these limitations, silicon-organic hybrid (SOH) platforms are proposed [2]. However, the bandwidths of SOH modulators are still narrower than expected due to large resistance induced by doped silicon strips or contacts [4]. On the other hand, although the compact footprints of silicon ring or disk modulators eliminate the need for travelling-wave design, the resonator photon life time sets an additional fundamental limit to the modulation speed [5].

Recent progresses in plasmonic technology greatly improve the optical-waveguide confinement capability and may provide a solution to the design of high speed electro-optic (EO) modulators. Several silicon-based plasmonic modulators have been theoretically proposed and fabricated [6], [7], [8], [9]. Although compact, the modulators in [6]–[9] suffer from high loss, low modulation efficiency, and challenges in manufacturing processes.

Here we propose a silicon-plasmonic hybrid racetrack ring modulator. As shown in Fig. 1(a), the modulator is based on a racetrack ring resonator coupled to a bus waveguide. An EO polymer infiltrated metal-dielectric-metal (MDM) waveguide is positioned above one straight-waveguide section of the racetrack ring with an insulating layer of silicon di-oxide, thus forming a hybrid phase shifter shown in Fig. 1(b). The signal voltage across the MDM slot can modulate the refractive index of the polymer through the Pockels effect. By introducing the ring structure, the length of the plasmonic waveguide can be shortened. The intrinsic modulation speed

of EO polymer can be ultrafast and the electrical signals are directly applied to the capacitor without transmission in the doped silicon strips, thus greatly reducing the  $RC$  time constant and also overcoming the limitation from free carrier effects in silicon.

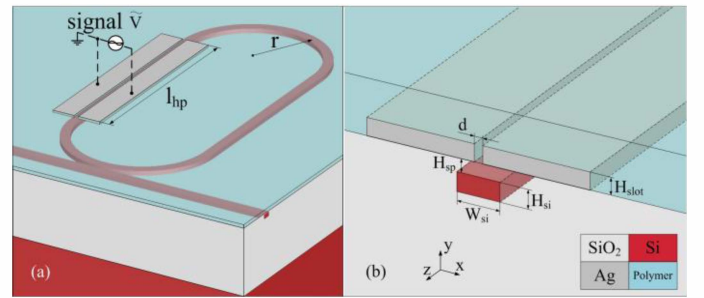


Figure. 1 Structure of the silicon-plasmonic hybrid modulator. (a) Perspective view of the racetrack ring resonator integrated with the MDM waveguide. (b) Perspective view of the silicon-plasmonic hybrid phase shifter.  $l_{hp}$ : length of the silicon-plasmonic hybrid phase shifter.  $r$ : radius of the racetrack ring.  $H_{sp}$ : height of the  $\text{SiO}_2$  space between the silicon waveguide and the metal plates.  $W_{si}$  and  $H_{si}$ : width and height of the silicon waveguide, respectively.  $d$  and  $H_{slot}$ : width and height of the slot, respectively.

## II. DEVICE DESIGN AND PARAMETER OPTIMIZATION

Based on coupled mode theory [10], the silicon waveguide photonic mode and MDM plasmonic mode in the hybrid phase shifter can be expressed as linear combinations of the quasi-even mode and quasi-odd mode as shown in Fig. 2(a) and (b), respectively. A small proportion of optical power also couples to radiation modes leading to additional losses, which are insignificant [11]. With  $n_e = n_e' + in_e''$  and  $n_o = n_o' + in_o''$  as the complex effective indices of the quasi-even mode and quasi-odd mode, respectively, the fraction of optical power coupled from the silicon waveguide to the MDM waveguide can be expressed as [10]

$$\eta = F \exp\left(\frac{-2z}{L_p}\right) \sin^2\left(\frac{\pi z}{2L_c}\right) \quad (1)$$

where  $F$  is the maximum fraction of coupled optical power,  $L_p$  and  $L_c$  are the mean attenuation and coupling length of the

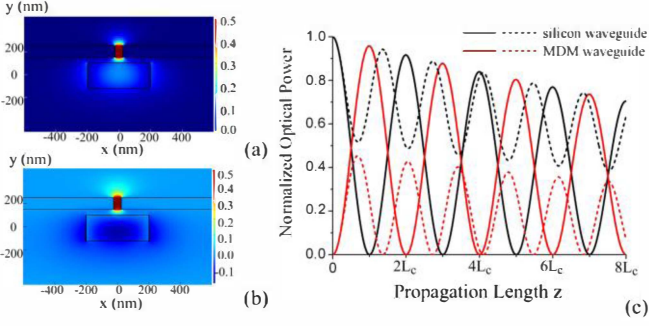


Figure 2  $E_x(x,y)$  component distributions of the quasi-even (a) and quasi-odd (b) TE modes supported by the silicon-plasmonic hybrid waveguide. (c) Normalized optical power inside the silicon waveguides (black curves) and the MDM waveguides (red curves) forming the silicon-plasmonic hybrid phase shifters. The solid and dashed curves correspond to the hybrid phase shifters satisfying and dissatisfying strong coupling conditions, respectively.

hybrid waveguide, respectively. Fig. 2(c) provides the normalized optical power inside the silicon waveguide (black curves) and the MDM waveguide (red curves) of the hybrid phase shifter, with strong coupling conditions [11] satisfied and dissatisfied, respectively. As shown in Fig. 2(c), the electric fields in both silicon and MDM waveguides exhibit alternative sinusoid fluctuations due to the beating between the quasi-even and quasi-odd modes. Under the strong coupling conditions,  $F \approx 1$ , which means that nearly all the power can be periodically coupled into and out of the MDM waveguide, thus optimizing the modulation effect when light interacts with the EO polymer inside the slot as shown by the solid curves in Fig. 2(c). Compared with plasmonic coupling schemes in [12], [13], such a silicon-plasmonic hybrid structure is non-resonant despite fabrication-induced defects and the optical power can be coupled back to the silicon waveguide when  $z = kL_c$  where  $k = 0, 2, 4$ , etc.

Fig. 3 shows the effective index real parts and the propagation losses for the quasi-even mode and quasi-odd mode as functions of silicon waveguide width  $W_{si}$  under different inserted  $\text{SiO}_2$  layer height  $H_{sp}$  and slot width  $d$ , respectively. Since  $L_c \approx \lambda / (2|n_e' - n_o'|)$ ,  $|n_e' - n_o'|$  should be large enough to obtain a small coupling length in order to design a compact device. Besides, the propagation loss and the fabrication feasibility need to be considered in choosing the dimensions of the silicon-plasmonic hybrid phase shifter.

The loss of a mode is determined by the proportion of its field localized inside the MDM waveguide. Under strong coupling conditions, both the quasi-even mode and quasi-odd mode have half of their fields concentrated on the MDM plasmonic waveguide, thus leading to the same loss [14], as marked by the intersection points A to C in Fig. 3(b). Hence,  $W_{si}$  can be set close to these intersection points to maximize the fraction of optical field coupled to the MDM waveguide.

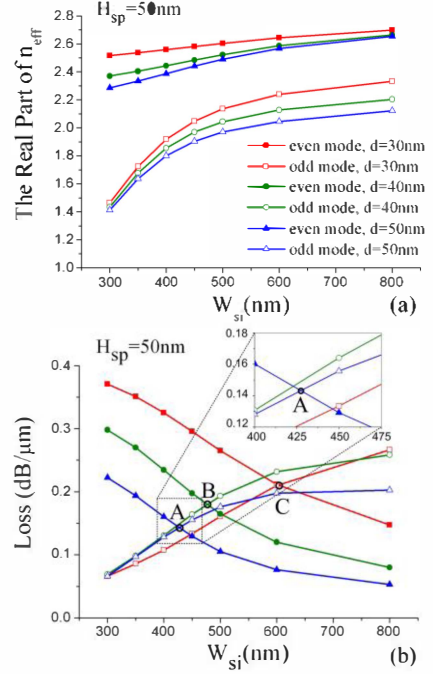


Figure 3 Effective index real parts and losses of the quasi-even and quasi-odd modes as functions of silicon waveguide width. The inset shows an enlarged figure of corresponding intersection points.  $H_{sp}$ : height of the  $\text{SiO}_2$  space between the silicon waveguide and the metal plates.  $d$ : MDM slot width.  $W_{si}$ : silicon waveguide width.

### III. MODULATION PERFORMANCE ANALYSIS

The transmission function at the output port of the bus waveguide under quasi-critical coupling condition can be deduced by multiple round-trip approach, as shown in Fig. 4. In order to satisfy round-trip phase matching requirement at 1550 nm, the corresponding parameters of the modulator are:  $W_{si} = 425$  nm,  $H_{si} = 220$  nm,  $H_{sp} = 50$  nm,  $d = 50$  nm,  $H_{slot} = 100$  nm,  $l = 34$   $\mu\text{m}$ , and  $l_{hp} = 8.36$   $\mu\text{m}$ .

We assume that the EO polymer achieves an EO coefficient,  $\gamma_{33}$ , of 150 pm/V at the wavelength of 1550 nm after an efficient poling process. The refractive index variation of the polymer under an applied voltage across the MDM slot,  $V$ , can be expressed as  $\Delta n = 0.5n_p^3\gamma_{33}V/d$ , where the refractive index of the polymer,  $n_p$ , is assumed to be 1.63. The phase-modulation speed is intrinsically very high due to the fast response of the Pockels effect. Fig. 4 shows the red-shifts and blue-shifts of the spectrum when  $n_p$  increases and reduces under positive and negative biases, respectively. As shown in Fig. 4, an extinction ratio of more than 15 dB can be achieved.

Several factors including RC time constant, photon life time, and driver electronics set limits to the modulation bandwidth of a ring modulator. Due to its compact size, the modulator can be regarded as a lumped element. The two parallel metal plates with the EO polymer sandwiched in between form a capacitor with  $C_m = \epsilon_0\epsilon_r A/d \approx 0.4$  fF, where  $\epsilon_0$  is the permittivity of vacuum,  $\epsilon_r = 2.657$  is the dielectric constant of EO polymer and  $A$  is the sidewall area of the metal

plates.

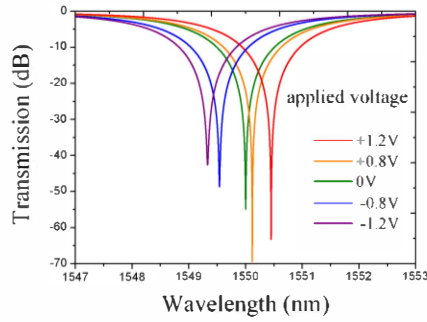


Figure. 4 Normalized transmission of the proposed modulator through port under different DC bias voltages across two parallel metal plates.

Given a typical value of loading resistance,  $R_m$ , of  $50 \Omega$  [6],  $1/R_m C_m$  is calculated on the order of terahertz, which may not be considered as a major restriction on the modulation speed.

The photon life time of a ring resonator,  $\tau_r$ , also sets a fundamental limit to the modulation bandwidth. Given the quality factor of the ring  $Q_r$ , one can obtain  $\tau_r = Q_r \lambda / (2\pi c)$  [5]. Due to the intrinsic loss induced by the MDM plasmonic waveguide, a decreased quality factor can be expected for the proposed device. As shown in Fig. 5,  $Q_r$  of the proposed modulator at 1550 nm is 510 leading to a calculated photon life time of 0.42 ps, which is smaller than the value of existing silicon ring modulators.

The power consumption can be estimated by  $P = C_m V^2 f / 2$  [6]. Given  $V = 2V$  and  $f = 100$  GHz,  $P/f$  is less than 10 fJ/bit which meets the energy efficient requirements in future SOI photonic circuits and terabit per channel optical communication networks.

#### IV. CONCLUSION

In this paper, a silicon-compatible plasmonic optical modulator is proposed. A silicon-plasmonic hybrid phase shifter clad with electro-optic polymer is integrated with a racetrack ring resonator to achieve high-speed performance and low energy consumption. Such a silicon-plasmonic hybrid modulator is promising for applications in future silicon inter-chip interconnects or ultrahigh-speed optical communication systems.

#### ACKNOWLEDGEMENT

This work was supported by National Natural Science Foundation of China (61077052/61125504), MoE

(20110073110012), and Science and Technology Commission of Shanghai Municipality (11530700400).

#### REFERENCES

- [1] H. Rong, A. Liu, R. Jones, O. Cohen, D. Hak, R. Nicolaescu, A. Fang, and M. Paniccia, "An all silicon Raman laser," *Nature*, vol. 433, pp. 292–294, Jan. 2005.
- [2] L. Alloatti, D. Korn, R. Palmer, D. Hillerkuss, J. Li, A. Barklund, R. Dinu, J. Wieland, M. Fournier, J. Fedeli, H. Yu, W. Bogaerts, P. Dumon, R. Baets, C. Koos, W. Freude, and J. Leuthold, "42.7 Gbit/s electro-optic modulator in silicon technology," *Opt. Exp.*, vol. 19, no. 12, pp. 11841–11851, Jun. 2011.
- [3] R. Ding, T. Baehr-Jones, Y. Liu, R. Bojko, J. Witzens, S. Huang, J. Luo, S. Benight, P. Sullivan, J.-M. Fedeli, M. Fournier, L. Dalton, A. K.-Y. Jen, and M. Hochberg, "Demonstration of a low  $V_\pi L$  modulator with GHz bandwidth based on electro-optic polymer-clad silicon slot waveguides," *Opt. Exp.*, vol. 18, no. 15, pp. 15618–15623, Jul. 2010.
- [4] T. Baehr-Jones, B. Penkov, J. Huang, P. Sullivan, J. Davies, J. Takayesu, J. Luo, T. Kim, L. Dalton, A. K.-Y. Jen, M. Hochberg, and A. Scherer, "Nonlinear polymer-clad silicon slot waveguide modulator with a half wave voltage of 0.25 V," *Appl. Phys. Lett.*, vol. 92, no. 16, Apr. 2008.
- [5] Q. Xu, V. R. Almeida, and M. Lipson, "Micrometer-scale all-optical wavelength converter on silicon," *Opt. Lett.*, vol. 30, no. 20, pp. 2733–2735, Oct. 2005.
- [6] W. Cai, J. S. White, and M. L. Brongersma, "Compact, high-speed and power-efficient electrooptic plasmonic modulators," *Nano Lett.*, vol. 9, no. 12, pp. 4403–4411, Oct. 2009.
- [7] S. Zhu, G. Q. Lo, and D. L. Kwong, "Electro-absorption modulation in horizontal metal-insulator-silicon-insulator-metal nanoplasmonic slot waveguides," *Appl. Phys. Lett.*, Vol. 99, no. 15, Oct. 2011.
- [8] J. A. Dionne, L. A. Sweatlock, M. T. Sheldon, A. P. Alivisatos, and H. A. Atwater, "Silicon-based plasmonics for on-chip photonics," *IEEE J. Sel. Topics Quantum Electron.*, vol. 16, no. 1, pp. 295–306, Jan. 2010.
- [9] S. Zhu, G. Q. Lo, and D. L. Kwong, "Theoretical investigation of silicon MOS-type plasmonic slot waveguide based MZI modulators," *Opt. Exp.*, vol. 18, no. 26, pp. 27802–27819, Dec. 2010.
- [10] G. Veronis and S. Fan, "Crosstalk between three-dimensional plasmonic slot waveguides," *Opt. Exp.*, vol. 16, no. 3, pp. 2129–2140, Feb. 2008.
- [11] C. Delacour, S. Blaize, P. Grosse, J. M. Fedeli, A. Bruyant, R. S. Montiel, G. Lerondel, and A. Chelnokov, "Efficient directional coupling between silicon and copper plasmonic nanoslot waveguides: toward metal-oxide-silicon nanophotonics," *Nano Lett.*, vol. 10, No. 8, pp. 2922–2926, Jul. 2010.
- [12] R. A. Wahsheh, Z. Lu, and M. A. G. Abushagur, "Nanoplasmonic couplers and splitters," *Opt. Exp.*, vol. 17, no. 21, pp. 19033–19040, Oct. 2009.
- [13] J. Tian, S. Yu, W. Yan, and M. Qiu, "Broadband high-efficiency surface-plasmon-polariton coupler with silicon-metal interface," *Appl. Phys. Lett.*, vol. 95, no. 1, Jul. 2009.
- [14] Q. Li and M. Qiu, "Structurally-tolerant vertical directional coupling between metal-insulator-metal plasmonic waveguide and silicon dielectric waveguide," *Opt. Exp.*, vol. 18, no. 15, pp. 15531–15543, Jul. 2010.